Flow-Around Airfoils with Blunt, Round, and Sharp Trailing Edges

B. E. Thompson*
Scientific Research Associates, Inc., Glastonbury, Connecticut
and
J. H. Whitelaw†
Imperial College of Science and Technology, London, England, United Kingdom

Attached and separated boundary layers were arranged on the suction side of a plate with a sharp trailing edge and compared to those around blunt and round trailing edges. Pressure and velocity characteristics were obtained with wall taps, impact probes, stationary and flying hot wires in the boundary layer, separated and wake flow regions. With the trailing plate inclined at 14 deg incidence and the boundary layer attached, the effect of the geometry of the trailing edge was confined to the near-wake region and was important mainly in the determination of base pressure. With the trailing plate at 17.5 deg incidence and turbulent boundary-layer separation, the structure of the separated and wake flow regions was significantly affected by the trailing-edge geometry. The results suggest that accurate calculation of lift, drag, and the onset of separation on airfoils as a function of incidence requires representation of the effects of trailing-edge shape and thickness on the pressure gradients in the direction across the boundary layer and in the streamwise direction, especially in the wake, on the turbulence structure of the backflow and, accordingly, on the rate of turbulence diffusion, upstream and downstream of the trailing edge, which determines the location and size of the recirculation region.

Nomenclature

Cp = pressure coefficient $p/\frac{1}{2}\rho U_{ref}^2$
s = distance from the leading edge tip wire
x = distance from the location of the sharp trailing edge. See Fig. 1.
z = spanwise distance from the centerline
δ = boundary-layer thickness ($U/Ue = .95$)

(Please also see Tables 1 and 2.)

Introduction

THE thickness and shape of the trailing edge of an airfoil has been identified as important to avert drag at high subsonic speeds,[1] to base-pressure drag[2] and, in some cases, lift,[2] to airfoil noise,[3] to the onset of shock-induced separation[4] and unsteadiness associated with shock movement and buffeting, to the separated flow region at high incidence,[5] to activation forces and moment on ailerons,[6] and to the development of the boundary-layer, separated, and wake flow regions of airfoils.[7] Although there is evidence for these effects, there is little information on the turbulence structure and boundary layer development in the vicinity of blunt or round trailing edges and with either attached or separated boundary-layer flow on the suction side. The experimental results presented here provide further understanding of the flow phenomena associated with the influence of trailing-edge shape.

Computational methods have been developed for turbulent separated flows based either on the solution of time-averaged Navier-Stokes equations throughout the flowfield[8-10] or on inviscid–viscous interactive techniques and the solution of boundary-layer and inviscid-flow equations.[11,12] Comparison of these approaches[13] suggests that there is not a distinct advantage for either approach. The Navier-Stokes approach is somewhat more suitable for extension to complex flow configurations, although there are uncertainties in numerical and turbulence-model assumptions. The interactive schemes are more efficient, but boundary-layer assumptions imply a limited range of applicability. Development of these methods requires verification with experimental results in flows reasonably similar to their practical application. It seems likely that the recirculation region in the vicinity of blunt or round trailing edges, which may be small but is apparently influential, affects the structure of the separated and wake flow to a degree that the assumptions in interactive and Navier-Stokes calculation methods require specific examination and verification by comparison with experimental results.

For the experiments on airfoils with blunt trailing edges discussed above, measurements of mean values of pressure and velocity obtained with impact probes have been reported. For example, Goradia et al.[5] obtained mean values of velocity, pressure, and skin friction in subsonic flow around a GA(W)-1 airfoil with a trailing-edge thickness of 2% of chord at a chord Reynolds number of about 1.1 million and at angles of incidence of 0, 6, 10, and 14 deg; and Cook and McDonald[7] measured mean pressure and velocity in the flow around a RAE 2822 airfoil with a trailing-edge thickness of 1.14% of chord at Reynolds numbers of about 2 and 5 million, Mach numbers of about 0.7 and angles of incidence of $-2.06, -2.45$ and -3.3 deg. Turbulence quantities were not reported.

Flow in the vicinity of sharp trailing edges has been measured for a range of angles of attack.[14-21] Thompson and Whitelaw,[19] Adair,[20] and Acharya et al.[21] obtained detailed measurements of the recirculating and attached flow over a sharp trailing edge at angles of incidence of 17.5, 16.0 and 14.2 deg, which resulted in a large region of recirculation, a small separated flow region and an attached suction side boundary-layer at the trailing edge, respectively. This paper represents an extension of their work to include blunt and round trailing edges which result in an additional region of recirculating flow due to the discontinuous change in surface shape. The evidence from the above three experiments is that the effects of recirculation on the mean flow and turbulence structure can be large, although the details of the backflow are unimportant, and suggests that interaction between the suction and pressure-side boundary layers and the backflow

Presented as Paper 87-0460 at the AIAA 25th Aerospace Sciences Meeting, Reno, NV; Jan. 12–15, 1987; received March 10, 1987; revision received Sept. 15, 1987.

*Research Scientist. Member AIAA.
†Professor of Convective Heat Transfer.

region associated with the discrete change in geometry at the trailing edge may be important, especially to the wake development.

The following section describes the flow configuration and measuring techniques. The Results and Discussion section discusses the results and their implications for calculation methods. The paper closes with a summary of the more important conclusions.

Experimental Investigation

The flow arrangement of Thompson and Whitelaw[19] was chosen so as to emphasize the flow characteristics in the trailing-edge region and avoid the complicating influences associated with leading-edge phenomena, such as transition or laminar separation bubbles. It comprised a 1 m flat plate, curved section of radius 0.8125 m and a trailing plate. The length of the curved section was adjusted so that the suction-side surface was at 14.2 and 17.5 deg incidence to the tunnel roof with the upstream plate at 0.3 and 1.0 deg incidence, respectively. These arrangements correspond to attached and separated boundary-layer flow, respectively, on the suction side near the trailing edge. The trailing-edge plate was arranged as shown in Fig. 1, with sharp 5 mm blunt and 5 mm round trailing edges. A thickness of 5 mm corresponds to a trailing-edge thickness of about 3.6% of the boundary-layer thickness at the trailing edge or about 0.33% of chord, with chord length defined as the distance from the trip wire to the sharp trailing edge along the suction-side surface. Table 1 shows the reference parameters which were chosen to enable comparison with the results of Thompson and Whitelaw[19] for the 17.5 deg incidence case, and Acharya et al.[21] for the 14 deg incidence case. The data are available in Ref. 27 for comparison purposes.

A region of two-dimensional mean flow extended over 90% of the span of the tunnel upstream of the curved section and reduced to a minimum of about 35% of tunnel span at the trailing edge, where the use of passive flow control vanes was required. Visualization with surface oil flow and smoke, and spanwise distributions of surface pressure and total pressure were used to assist adjustment of the vanes to maximize the region of two-dimensional flow. Figure 2 shows the cross-section distributions of static pressure on the wall near the trailing edge which show a region of pressure gradient less than 3 and 4% of the local streamwise pressure gradient for the 17.5 and 14 deg cases, respectively. In this region, the

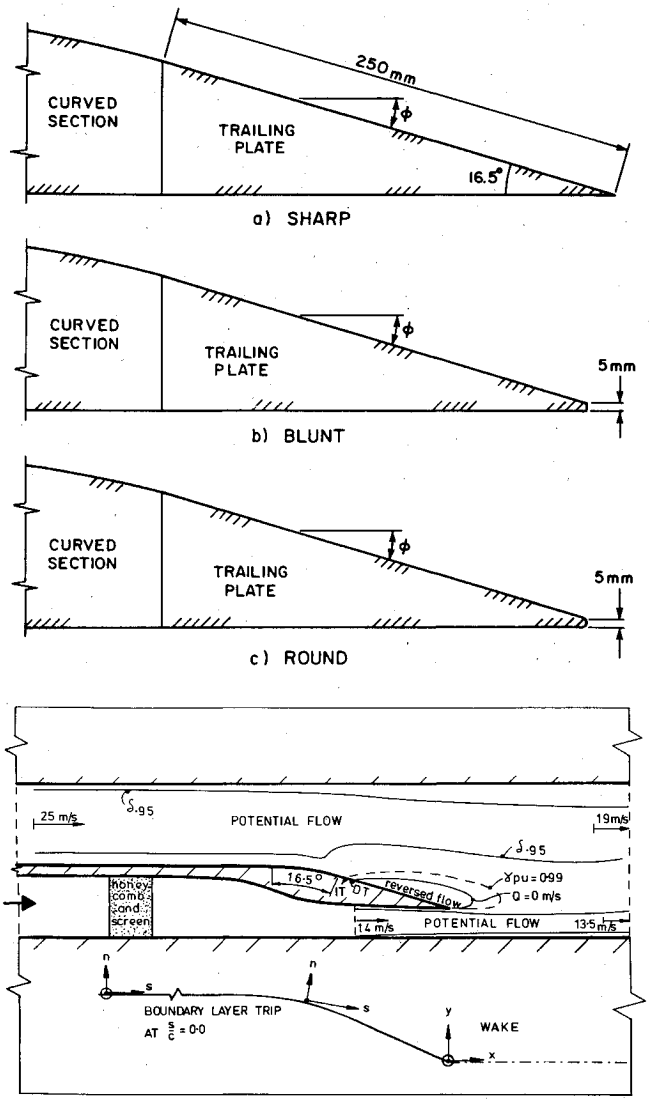

Fig. 1 Flow configuration.

Table 1 Reference parameters

Parameter [symbol]	Value
Viscosity [ν]	15.2×10^{-6} m^2/s
Density [ρ]	1.2 kg/m^3
Temperature [T]	20°C
14.2 deg incidence	
Velocity [U_{ref}]	25.0 m/s
Chord length [C]	1.439 m
Static pressure relative to atmospheric [P_{ref}]	-156 N/m^2
Reynolds number $\left[\mathrm{Re} = \frac{U_{ref} C}{\nu}\right]$	2.4×10^6
17.5 deg incidence	
Velocity [U_{ref}]	26.3 m/s
Chord length [C]	1.518 m
Static pressure relative to atmospheric [P_{ref}]	-207 N/m^2
Reynolds number $\left[\mathrm{Re} = \frac{U_{ref} C}{\nu}\right]$	2.6×10^6

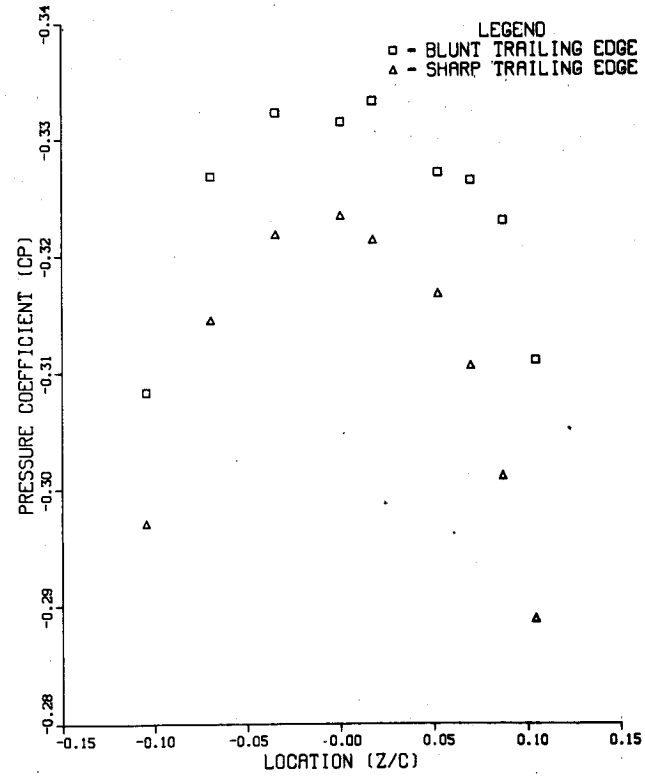

Fig. 2a Spanwise surface pressure distribution at S/C of 0.928.

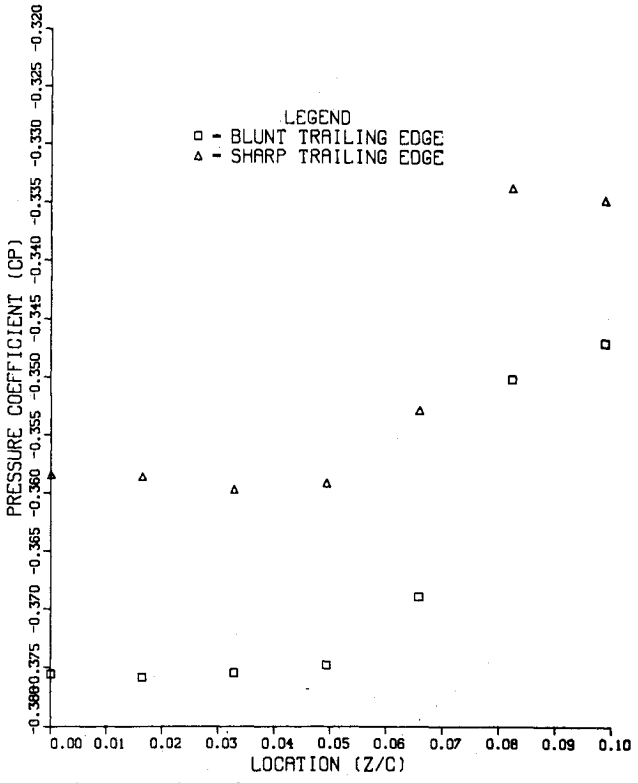

Fig. 2b Spanwise surface pressure distribution at S/C of 0.932.

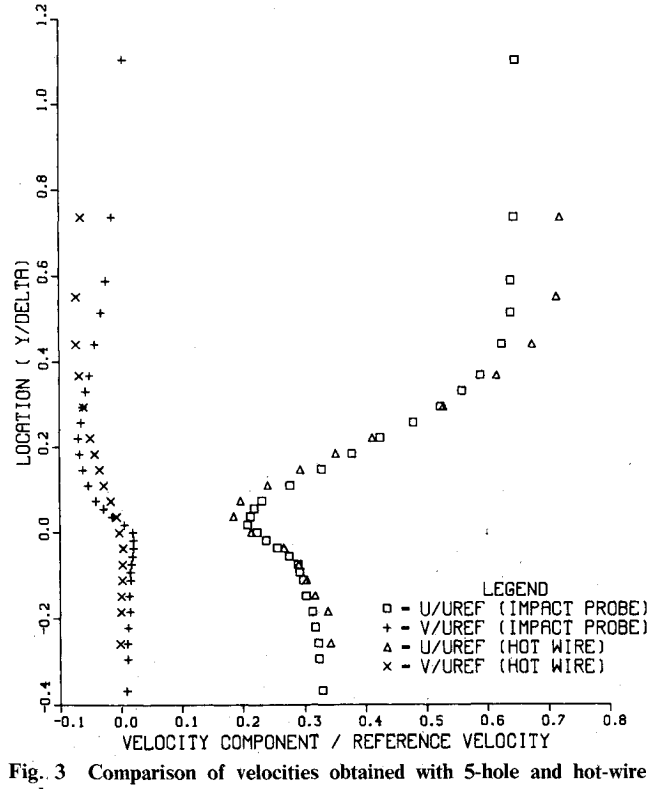

Fig. 3 Comparison of velocities obtained with 5-hole and hot-wire probes.

surface oil flow and smoke patterns appeared two-dimensional in the mean and the spanwise distribution of total pressure was measured to be constant within 2% at locations above 0.1 boundary-layer thickness. Terms in the momentum-integral equation for two-dimensional subsonic flow with significant normal pressure gradient were evaluated using second-order-accurate methods for the integrals and derivatives and using the logarithmic law of the wall for the skin friction and

Table 2 Maximum uncertainty in hot-wire measurements

Stationary hot-wire anemometry		
Mean velocity magnitude	$\langle U \rangle$	0.3 m/s
Flow angle	$\langle \theta \rangle$	0.4 deg
Reynolds stresses	$\langle u^2 \rangle$	3% of $\langle U \rangle^2$
	$\langle v^2 \rangle$	10% of $\langle U \rangle^2$
	$\langle uv \rangle$	7% of $\langle U \rangle^2$
Flying hot-wire anemometry		
Mean velocity magnitude	$\langle U \rangle$	0.35 m/s
Flow angle	$\langle \theta \rangle$	0.6 deg
Reynolds stresses	$\langle u^2 \rangle$	7% of $\langle U \rangle^2$
	$\langle v^2 \rangle$	20% of $\langle U \rangle^2$
	$\langle uv \rangle$	14% of $\langle U \rangle^2$

velocity variation near the wall. The balance was within 6% of the largest term in the regions of the upstream boundary layer approaching separation and the wake, including locations which were 50 mm away from the centerline. The largest discrepancies occurred in the immediate vicinity of mean-streamline detachment and just downstream of the trailing edge and this may be attributed largely to variations in the static pressure caused by flow-curvature effects associated with separation.

Surface pressure was obtained from wall taps of 0.5 mm internal diameter which were arranged in accordance with the recommendations of Chue.[22] The maximum uncertainty in wall pressure measurements was accordingly less than 0.0035 of Cp.

Distributions of mean values of static pressure and mean velocity across the boundary layer and wake were obtained with a five-hole impact probe that had a maximum cross-flow dimension of 2.58 mm and was calibrated and operated following the procedures recommended by Bryer and Pankhurst.[23] The velocity results obtained with the five-hole impact probe and the hot-wire anemometer are shown in Fig. 3 and are in agreement in regions of small total-pressure gradient. The total-pressure gradient across the impact probe in the shear layers close to the wall and in the wake resulted in velocity measurements from the five-hole and hot-wire probes that differed by less than 2.5 and 1.5 m/s in streamwise and cross-stream velocity components, respectively. This corresponds to a maximum uncertainty in Cp of less than 0.034.

Constant-temperature hot-wire anemometry was used to obtain velocity characteristics in regions of attached boundary-layer and wake flow outside of regions of reversing flow where flying-wire anemometry was required. Cross-wire probes (DISA 55P61) with 5 μm diam heated wire sensors arranged in the plane perpendicular to the airfoil surface were used with constant-temperature bridges (DISA 55M10) at an overheat ratio of 1.8 and a frequency response in excess of 100 KHz. The hot-wire voltage was converted to a 12-bit digital signal with an analog-to-digital converter (DEC AD01) and sample-and-hold modules (analogic MP 240) and recorded by computer (DEC PDP8E). Voltages were converted to effective cooling velocity with the explicit calibration curve of Thompson and Whitelaw.[24] Ensemble averages of wire-cooling velocity were determinable within the accuracy specified on Table 2. Transformation of the effective cooling velocity to flow velocity characteristics was performed with a method based on the curve-fitting procedure of Ribeiro[25] and is described by Thompson.[26]

The flying hot-wire anemometer of Thompson and Whitelaw[24] was used to measure velocity characteristics of the flow in and around recirculation regions where negative values of instantaneous velocity occur. The wire trajectory began from a rest position located outside the boundary layer and was accelerated until it attained a predetermined maximum velocity of up to 15 m/s. This velocity was maintained as the probe passed through the flow region of interest, where instantaneous values of effective wire-cooling velocity were recorded

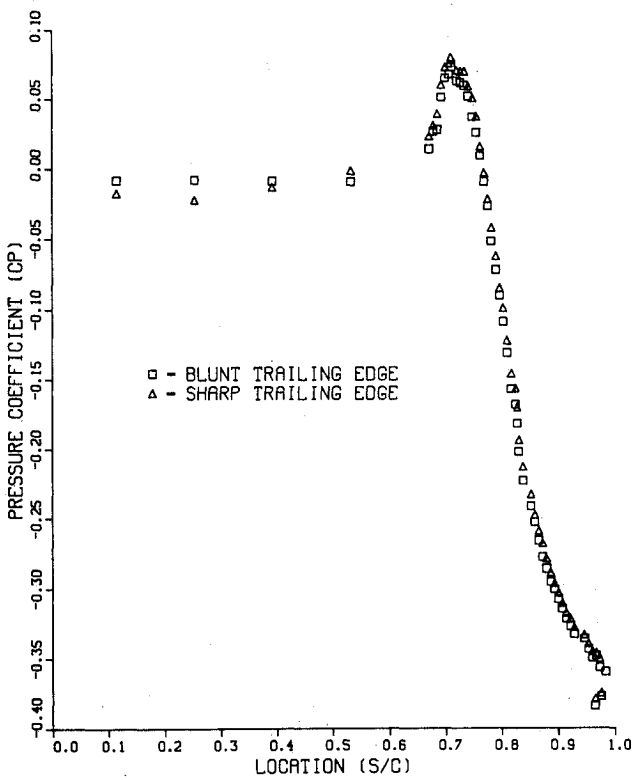

Fig. 4a Centerline surface pressure distribution at 14.2 deg incidence. □ Blunt; △ Sharp.

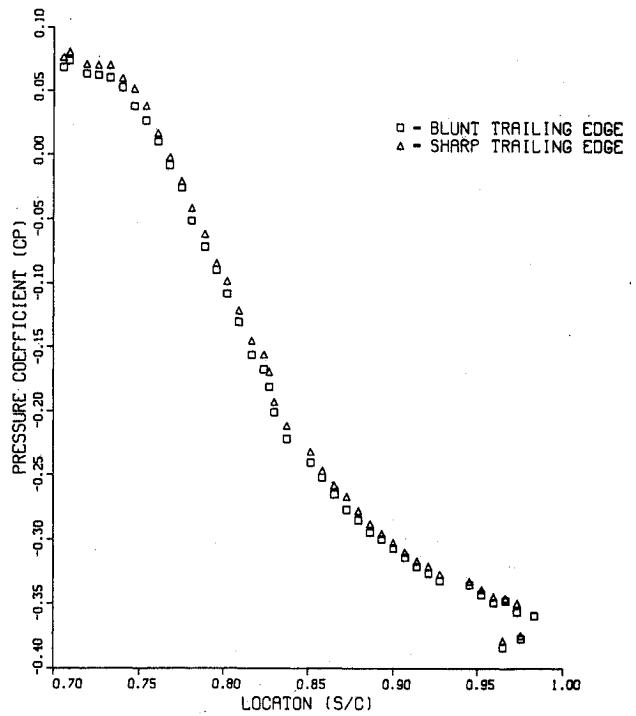

Fig. 4b Centerline surface pressure distribution at 14.2 deg incidence. □ Blunt; △ Sharp.

at a series of preselected locations along the probe trajectory. The momentum of the wire mechanism carried the probe back to the rest position where it remained until any disturbances affecting the flow in the region of interest were dissipated, which for the present flow was about 20 s, after which another series of velocity values were obtained.

Maximum uncertainties for the velocity results obtained with stationary and flying hot-wire anemometry are shown in Table 2. The velocity characteristics obtained with the hot

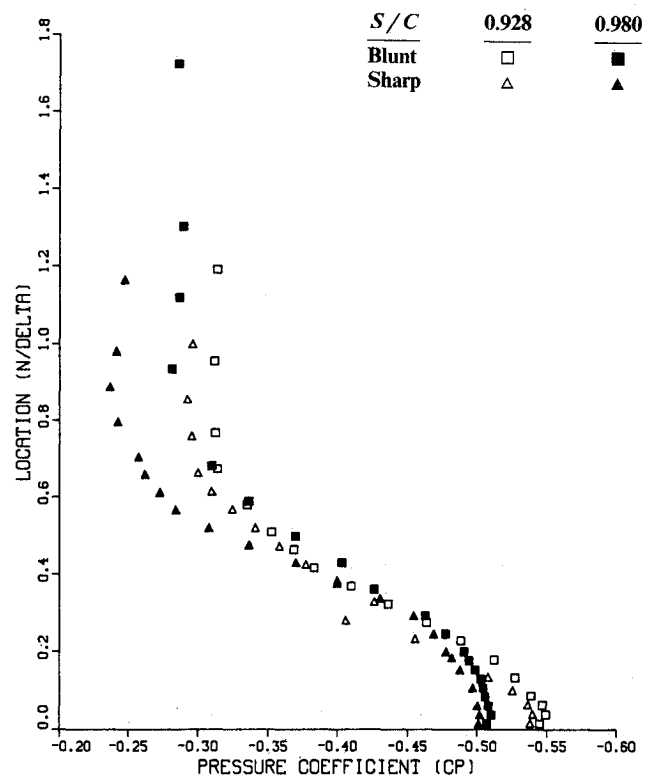

Fig. 5a Distributions of static pressure coefficient at 14.2 deg incidence.

wires were subject to smaller uncertainties associated with velocity gradients across the probe sensor than those obtained with impact probes and, accordingly, were preferred in the figures below.

Results and Discussion

Experimental results are presented in the flow around the sharp, blunt, and round trailing-edge configurations of Fig. 1. Two arrangements of the suction-side surface are considered: the trailing-edge plate is inclined at angles of incidence of 14 and 17.5 deg relative to the tunnel walls and the resulting boundary layers are attached and separated, respectively, as they leave the suction-side surface at the sharp trailing edge.

Distributions of static pressure coefficient on the centerline of the surface at 14 deg incidence are shown in Fig. 4. The surface pressure distribution is independent of the shape of the trailing edge up to the location where the trailing edge was cut off. With the sharp trailing edge, the pressure and suction-side boundary layers remain attached until they leave the trailing edge and with the blunt and round cases, the location of separation, which was identified with smoke visualization, appears to be located at the sharp corner or at about the discontinuity in surface curvature, respectively. The cross-stream and downstream length of these recirculation bubbles was about 0.035 and 0.04% of chord, respectively.

The distribution of static pressure coefficient, velocity ratio, and Reynolds stresses of Figs. 5, 6, and 7 for the trailing plate at 14 deg incidence shows that there is little difference between the flow around the blunt and sharp trailing edges, except in the near wake. Upstream of the location where the trailing edge was cut off, the distributions of mean values of pressure, velocity, and turbulence intensity were in agreement and indicate a negligible upstream effect of the modification to the trailing edge. In the wake downstream of about x/c of 0.045, the distributions of mean and turbulence quantities are also in agreement, and the rate of recovery is independent of the trailing-edge shape. In the region between the trailing edge and x/c of 0.12, there are differences between the sharp, blunt, and round trailing-edge flows which are associated with

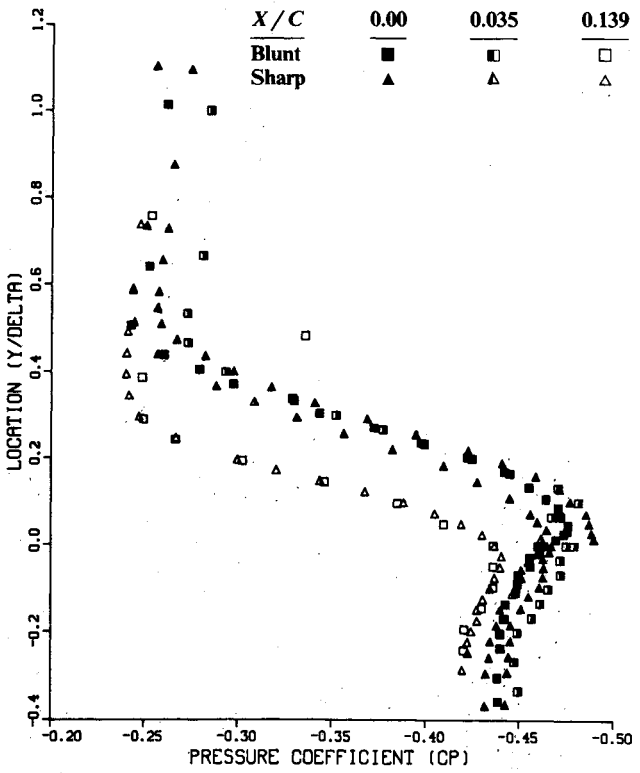

Fig. 5b Distributions of static pressure coefficient at 14.2 deg incidence.

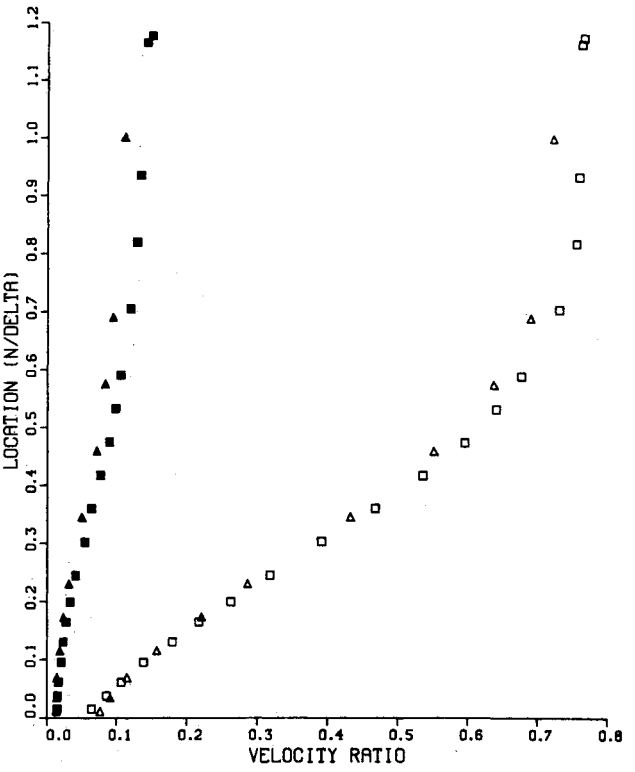

Fig. 6b Distributions of mean velocity S/C of 0.980.

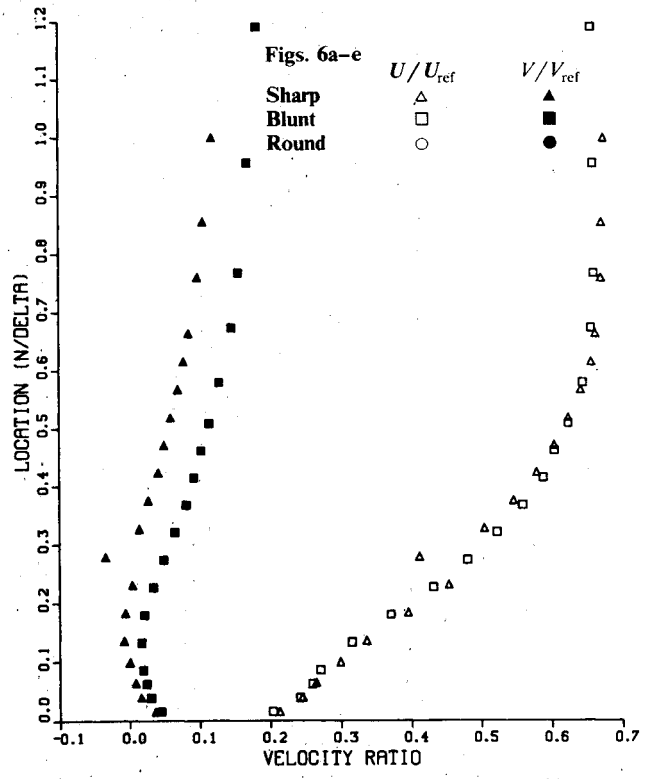

Fig. 6a Distributions of mean velocity S/C of 0.928.

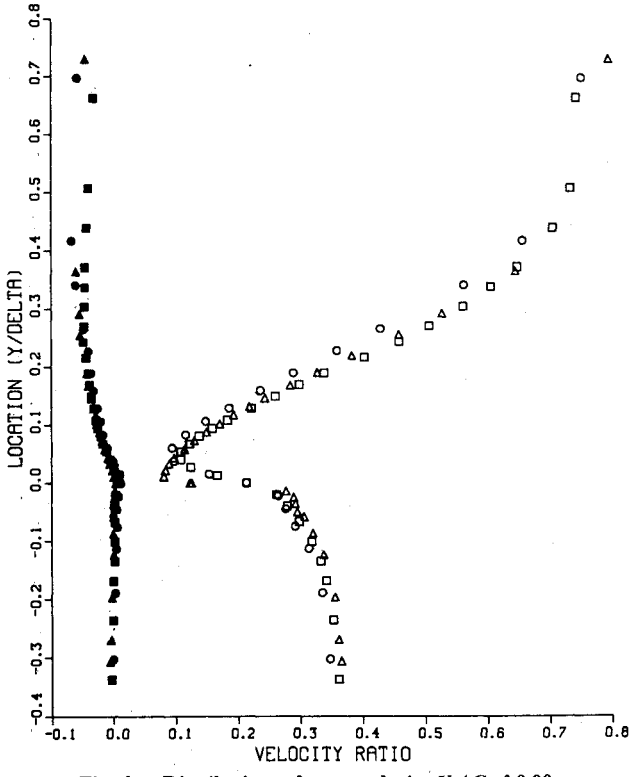

Fig. 6c Distributions of mean velocity X/C of 0.00.

differences in the small recirculating flow region observed with smoke visualization. The mean velocity distribution between y/δ of -0.04 and 0.05, with δ defined as the boundary-layer thickness where the mean velocity reaches 99% of its freestream value, is affected by the shape of the trailing edge. Reynolds normal and shear stress values in the near wake were measured to be larger than in the attached boundary-layer flow upstream. The effect of the blunt trailing edge was to increase the values of the Reynolds stresses just downstream of the trailing edge by amounts larger than with the sharp trailing edge, with those obtained with a round trailing edge in between. Different values of Reynolds stresses in the very near wakes downstream of the sharp, round, and blunt trailing edges are a consequence of the different rates of turbulence production associated with interaction of the boundary layers and, in the blunt and round trailing-edge cases, with the

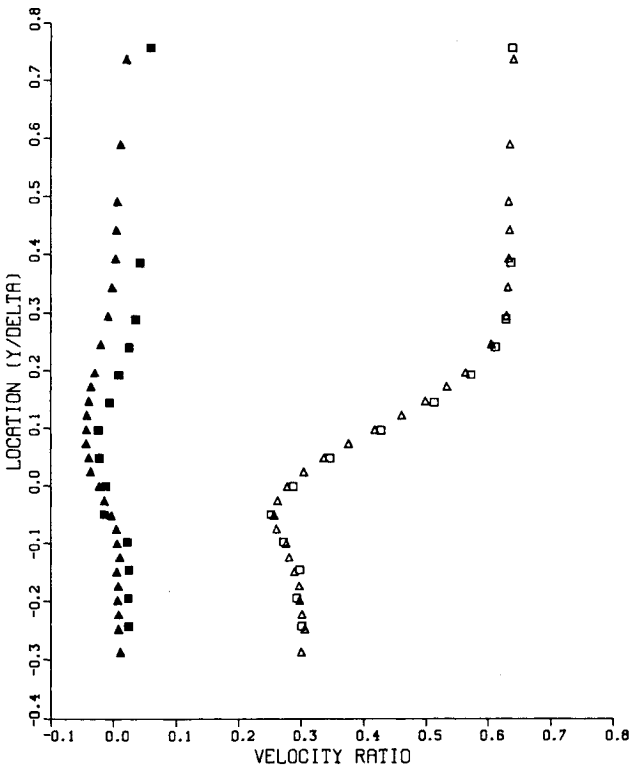

Fig. 6d Distributions of mean velocity X/C of 0.035.

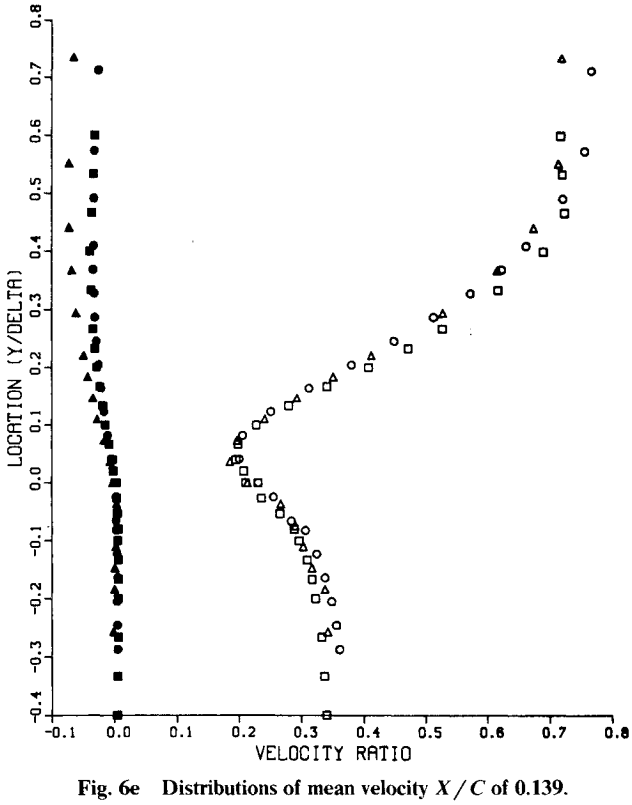

Fig. 6e Distributions of mean velocity X/C of 0.139.

recirculation regions just downstream of the trailing edge. The effects, which include those on the mean flow and turbulence, are, however, confined to the very near wake. Even at distances of about x/c of 0.042 downstream of the trailing edge, there is little influence of trailing-edge shape on the wake development.

Figure 8 shows the distribution of static pressure on the suction-side surface for the angle of incidence of 17.5 deg, with blunt and sharp trailing edges. In contrast to the arrangement at 14 deg incidence, there is an important effect of the trailing-edge shape on the pressure distribution upstream of the trailing edge. Surface oil-flow visualization showed that the location of mean streamline detachment with the blunt trailing edge was about 1.2% of chord upstream of that with the sharp trailing edge, where it was at s/c of 0.87. Accordingly, the surface pressure distribution shows different rates of pressure recovery from s/c of about 0.82 downstream to the almost constant values in the recirculating flow. Values of surface pressure in the recirculation region are more negative with the blunt trailing edge which is consistent with a larger region of recirculation.

The distribution of static pressure across the wake flow at s/c of 0.13 downstream of rear stagnation point of the recirculating flow is shown in Fig. 9 for the trailing plate at 17.5

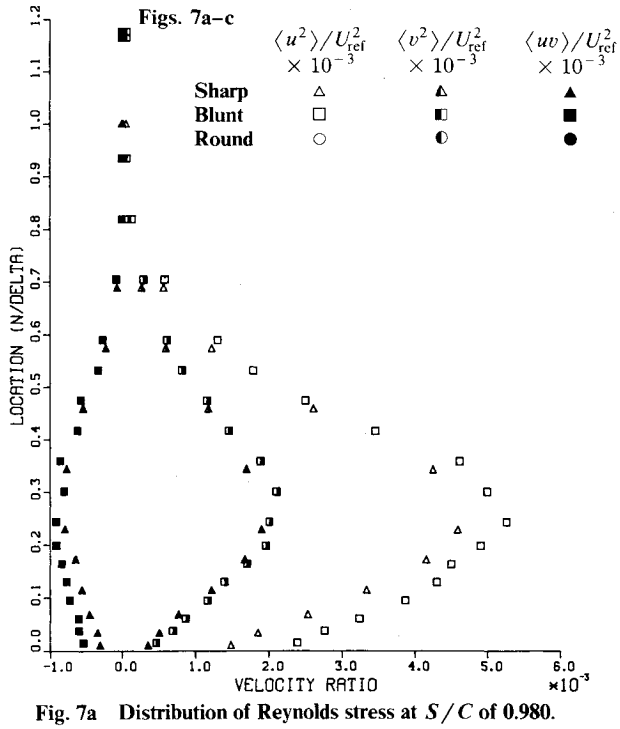

Fig. 7a Distribution of Reynolds stress at S/C of 0.980.

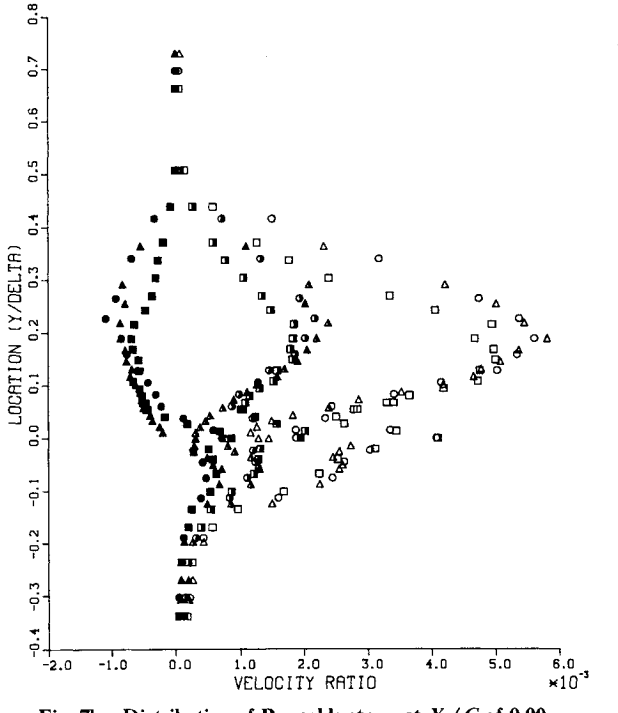

Fig. 7b Distribution of Reynolds stress at X/C of 0.00.

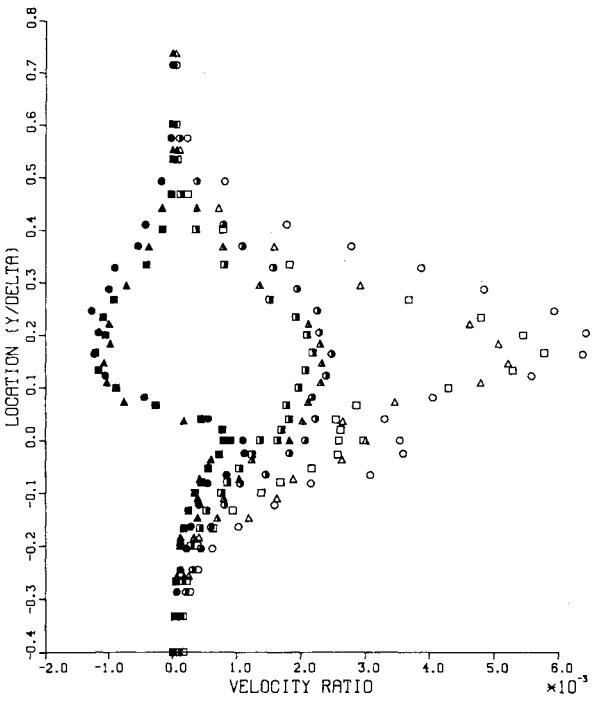

Fig. 7c Distribution of Reynolds stress at X/C of 0.035.

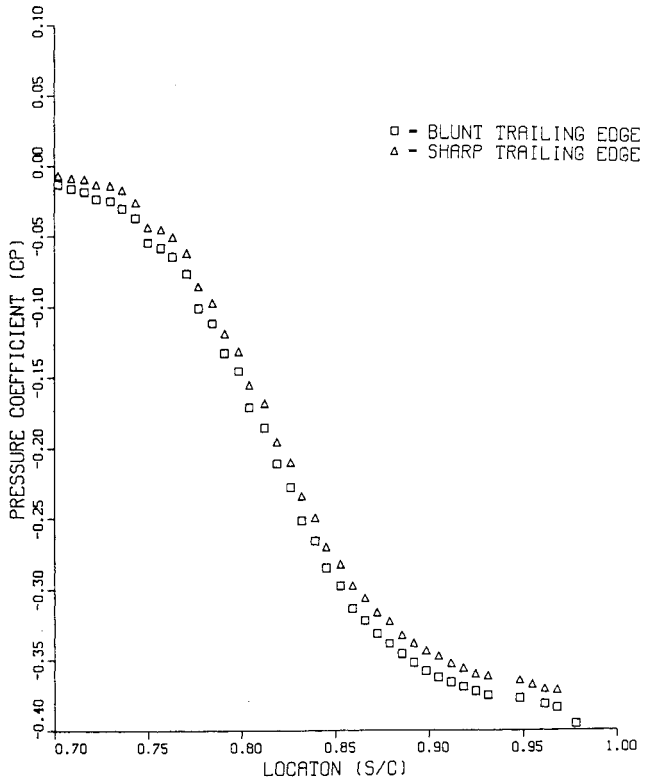

Fig. 8a Centerline surface pressure distribution at 17.5 deg incidence. □ Blunt; △ Sharp.

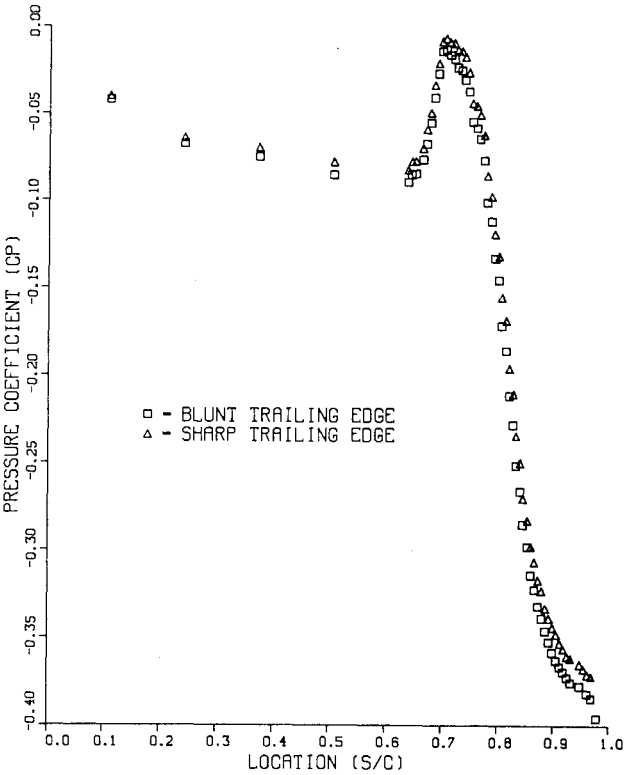

Fig. 8b Centerline surface pressure distribution at 17.5 deg incidence. □ Blunt; △ Sharp.

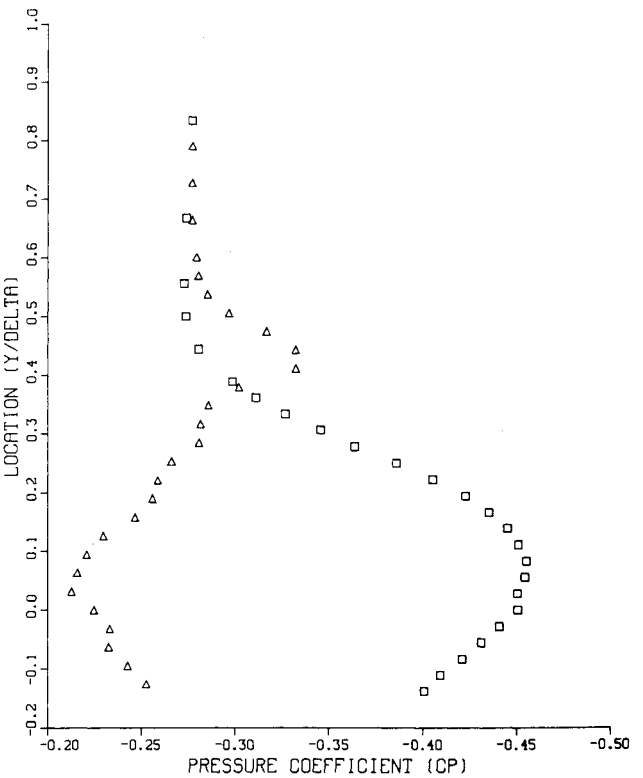

Fig. 9 Distribution of static pressure coefficient at 17.5 deg incidence at X/C of 0.132.

deg incidence. The agreement between Cp obtained with sharp and blunt trailing edges is within 0.04 and suggests that the flow with the larger recirculation, that is with the blunt trailing edge, recovers more rapidly with downstream distance and that the blunt trailing edge affects increases to the upstream extent of the recirculating flow.

Figures 10 and 11 show mean velocity and Reynolds shear stress results in the recirculating flow and wake obtained with a combination of stationary and flying hot-wire anemometry with the trailing plate at 17 deg incidence. Larger values of the Reynolds shear stress and differences in the mean velocity distributions are consistent with the larger region of recirculation caused by the blunt trailing edge.

Flow visualization and near-wall measurements with the flying hot wire indicate a small secondary recirculation region at the start of the reversed flow boundary layer just upstream

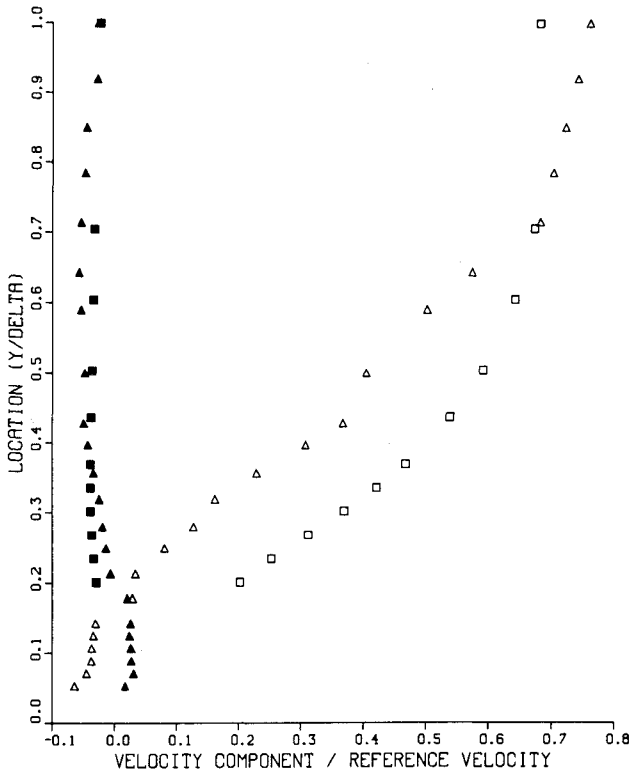

Fig. 10a Distribution of mean velocity at 17.5 deg incidence at X/C of 0.00. Symbols as shown in Fig. 6.

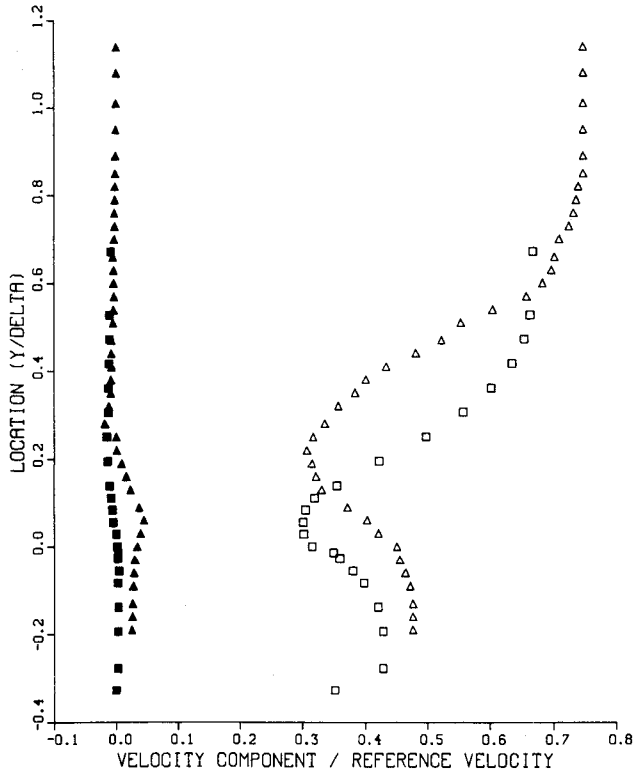

Fig. 10b Distribution of mean velocity at 17.5 deg incidence at X/C of 0.132. Symbols as shown in Fig. 6.

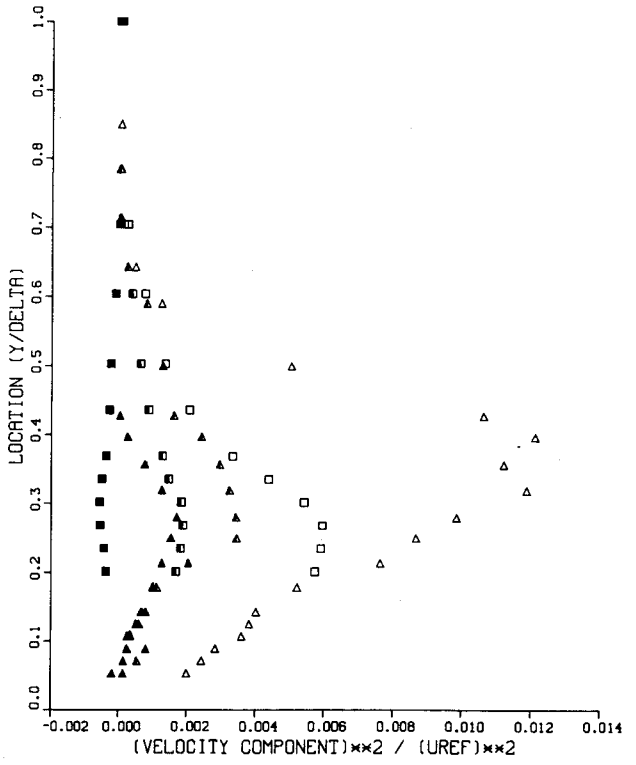

Fig. 11a Distribution of Reynolds stresses at X/C of 0.00. Symbols as shown in Fig. 7.

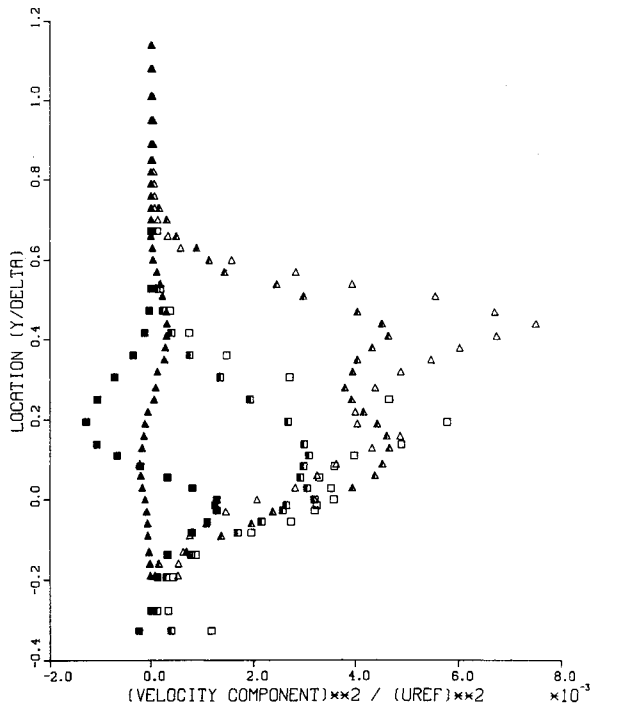

Fig. 11b Distribution of Reynolds stresses at X/C of 0.132. Symbols as shown in Fig. 7.

of the trailing edge. This secondary backflow recirculation region may be a consequence of the backflow being forced around the sharp edge of the blunt trailing edge as it moves forward, due to the adverse pressure gradient, toward the point of mean streamline detachment. It appears that this secondary recirculation increases the turbulence intensity in the recirculating flow with the blunt trailing edge and makes a substantial contribution to the production of turbulence energy close to the wall. Further measurements are needed to quantify fully the secondary recirculation.

For blunt, sharp, and round trailing-edge flow where the boundary layer remains attached to the end of a sharp trailing edge, it seems adequate to represent the effects of the finite trailing-edge thickness by extending the surface streamlines until they intersect in the wake. For the purposes of the boundary-layer calculation, the base pressure may be taken as

the average of the pressure and suction-side values at the location where the airfoil is truncated, for the calculation of lift and form drag. However, for calculation procedures that attempt to represent the onset of separation or the recirculating flow, there will need to be some account of the influence of trailing-edge shape which appears to have an influence upstream on the initial stages of development of the reverse flow boundary layer and thus the structure and size of the backflow region. The scale of the flow in this region, which includes the secondary recirculation discussed above, is small compared to the scale of the boundary-layer or outer inviscid flow. Small mesh spacing will be required in the vicinity of the trailing edge or some type of empirical correlation based on experimental results may be devised.

Concluding Remarks

The influence of the trailing-edge shape was found to be local to the near-wake region from the trailing edge to about 4.5% of chord downstream for flows with angle of incidence arranged so that the boundary layer remains attached over a sharp trailing edge. The pressure distribution and boundary-layer structure on the suction and pressure-side surfaces was independent of trailing-edge shape and the base pressure was about equal to the average of the pressures on suction and pressure-side surfaces at the discontinuous change in surface geometry with blunt and round trailing edges. There is experimental evidence of a recirculation region that extended 0.04% of chord into the near wake with the blunt and round trailing-edge configurations, which was not present when a sharp trailing edge was used and the boundary layers remained attached to the surface. Differences between the flow around sharp, blunt, and round trailing edges were not, however, observed 4.5% of chord downstream of the trailing edge and were not important to the overall flow patterns.

When the boundary layer was arranged to separate upstream of a sharp trailing edge, the influence of trailing-edge shape increased the size and affected the structure of the recirculation region on the suction side. The location of mean streamline detachment with a blunt trailing edge was upstream of that with a sharp trailing edge by about 1.2% of chord and was accompanied by an increase in the dimensions of the recirculation region and boundary-layer thickness of about 5 and 1%, respectively. There appeared to be a small secondary recirculation in the backflow on the suction side surface at the trailing edge. The blunt trailing edge increased the Reynolds stresses and affected the mean flow and turbulence structure of the backflow and this, combined with the larger strain rates associated with a larger recirculation bubble, increased the rate of recovery in the wake by about 5%. Lift coefficient and stall angle of an airfoil at high angle of attack would likely decrease with a blunt trailing edge, because deflection of the mean flow is larger around the recirculation region associated with the blunt trailing edge, although the greater recovery rate in the wake may decrease the base drag and interfere less with trailing flaps.

The effects of trailing-edge shape need to be represented in calculations of mean-flow and turbulence quantities that attempt to predict turbulent boundary-layer separation. Empirical methods or very fine calculation meshes are suggested to represent the small recirculation regions in the vicinity of the trailing edge.

Acknowledgments

Financial support from the S.E.R.C. of the United Kingdom and N.S.E.R.C. of Canada is gratefully acknowledged. Dr. B.R. Williams of the Royal Aircraft Establishment and Mr. B. Eggleston of the de Havilland Aircraft of Canada Limited are also thanked for advice given in many useful discussions.

References

[1] Whitcombe, R.T. and Heath, A.R., "Several Methods for Reducing the Drag of Transport Configurations at High Subsonic Speeds," NASA Memo 225-59L, 1959.

[2] Tanner, M., "Reduction of Base Drag," *Progress in Aerospace Science*, Vol. 6, 1975, p. 369.

[3] Chou, S.-T. and George, A.R., "Effect of Blunt Trailing Edge on Rotor Broadband Noise," *AIAA Journal*, Vol. 24, Aug. 1986, p. 1380.

[4] Pearcey, H.H., "Some Effects of Shock-Induced Separation of Turbulent Boundary Layers in Transonic Flow Past Airfoils," ARCR&M 3108, 1955.

[5] Goradia, S.H., Mehta, J.M., and Shrewsbury, G.S., "Analyses of the Separated Boundary Layer Flow on the Surface and in the Wake of Blunt Trailing Edge Airfoils," NASA CR 145202, 1977.

[6] Hoerners, S.F. and Borst, H.B., "Fluid Dynamic Lift," Hoerner Publishers, New Jersey, 1975.

[7] Cook, P.H. and McDonald, M.A., "Wind Tunnel Measurements in the Boundary Layer and Wake of an Aerofoil with a Blunt Base at High Subsonic Speeds," RAE TR 84002.

[8] Shamroth, S.J., "Calculation of Steady and Unsteady Airfoil Flow Fields Via the Navier-Stokes Equations," NASA CR 3899.

[9] Reis, L. and Thompson, B.E., "Comparison of Finite-Difference Calculations of a Large Region of Recirculating Flow Near an Airfoil Trailing Edge," AGARD CP412, Paper 19.

[10] Rhie, C.M. and Chow, W.L., "A Numerical Study of the Turbulent Flow Past an Isolated Airfoil with Trailing Edge Separation," *AIAA Journal*, Vol. 21, 1982, p. 1525.

[11] Williams, B.R., "The Prediction of Separated Flow Using a Viscous-Inviscid Interaction Method," Proceedings of the 14th ICAS Congress, Toulouse, France, 1984.

[12] McDonald, H. and Briley, W.R., "A Survey of Recent Work on Interacted Boundary Layer Theory for Flow with Separation," Numerical and Physical Aspects of Aerodynamic Flows, II, edited by T. Cebeci, Springer-Verlag, 1983, p. 141.

[13] Adair, D., Thompson, B.E., Whitelaw, J.H., and Williams, B.R., "Comparison of Interactive and Navier-Stokes Calculations of Separating Boundary-Layer Flows," Numerical and Physical Aspects of Aerodynamic Flows, III, edited by T. Cebeci, Springer-Verlag, 1985, p. 168.

[14] Brooks, T.F., Marcolini, M.A., and Pope, D.S., "Airfoil Trailing-Edge Flow Measurements," *AIAA Journal*, Vol. 24, Aug. 1986, p. 1245.

[15] Nakayama, A., "Characteristics of the Flow Around Conventional and Supercritical Airfoils," *Journal on Fluid Mechanics*, Vol. 160, 1985, p. 155.

[16] Nakayama, A., "Measurement of Attached and Separated Flows in the Trailing-Edge Region of Airfoils," Numerical and Physical Aspects of Aerodynamic Flows, II, edited by T. Gebeci, Springer-Verlag, 1984, p. 233.

[17] Viswanath, P.R., Cleary, J.W., Seegmiller, H.L., and Horstman, C.C., "Trailing-Edge Flows at High Reynolds Number," *AIAA Journal*, Vol. 18, Aug. 1980, p. 1059.

[18] Viswanath, P.R. and Brown, J.L., "Separated Trailing-Edge Flow at a Transonic Mach Number," *AIAA Journal*, Vol. 21, June 1983, p. 803.

[19] Thompson, B.E. and Whitelaw, J.H., "Characteristics of a Trailing Edge Flow with Turbulent Boundary Layer Separation," *Journal of Fluid Mechanics*, Vol. 157, 1985, p. 305.

[20] Adair, D., "Characteristics of a Trailing Flap Flow with Small Separation," Fluids Section Rept. FS/85/12, Imperial College, London, England. *Experiments in Fluids,* Vol. 5, 1987, p. 114.

[21] Acharya, S., Adair, D., and Whitelaw, J.H., "Flow Over a Trailing Flap and Its Asymmetric Wake," Fluids Section Report FS/85/26, Imperial College, London, 1985.

[22] Chue, S.H., "Pressure Probes for Fluid Measurement," Prog. Aero. Sci., Vol. 16, 1975, p. 146.

[23] Bryer, D.W. and Pankhurst, R.C., "Pressure Probe Methods for Determining Windspeed and Flow Direction," Her Majesty's Stationary Office, London, 1971.

[24] Thompson, B.E. and Whitelaw, J.H., "Flying Hot Wire Anemometry," *Experiments in Fluids*, Vol. 2, 1984, p. 47.

[25] Ribeiro, M.M., "The Turbulence Structure of Free Jet Flows With and Without Swirl," Ph.D. Thesis, University of London, London.

[26] Thompson, B.E., "The Turbulent Separating Boundary Layer and Its Downstream Wake," Ph.D. Thesis, Univ. of London, London.

[27] Thompson, B.E. and Whitelaw, J.H., "Attached and Separated Boundary-Layer Flow Around Airfoils with Blunt, Round and Sharp Trailing Edges," Imperial College Fluid Section Rept. FS/86/20, Imperial College, Dept. of Mechanical Engineering, 1986.